Group 3: Outskirts of nearby galaxies

https://doi.org/10.1017/S1743921316012291 Published online by Cambridge University Press

Formation and Evolution of Galaxy Outskirts
Proceedings IAU Symposium No. 321, 2016
A. Gil de Paz, J.H. Knapen & J.C. Lee, eds.

doi:10.1017/S1743921316012291

Probing Galactic Outskirts with Dragonfly

Roberto Abraham[1,2], Allison Merritt[3], Jielai Zhang[1,2,4], Pieter van Dokkum[3], Charlie Conroy[5], Shany Danieli[3,5,6,7] and Lamiya Mowla[3]

[1]Department of Astronomy and Astrophysics, University of Toronto
[2]Dunlap Institute for Astronomy and Astrophysics, University of Toronto
[3]Department of Astronomy, Yale University
[4]Canadian Institute for Theoretical Astrophysics
[5]Harvard-Smithsonian Center for Astrophysics
[6]Department of Physics, Yale University
[7]Yale Center for Astronomy and Astrophysics

Abstract. We describe the challenges inherent to low surface brightness imaging and present some early results from the Dragonfly Nearby Galaxies survey. Wide field, ultra-low surface brightness imaging ($\mu_g > 31$ mag arcsec^{-2}) of the first eight galaxies in the survey reveals a rich variety in the distribution of stars in the outskirts of luminous nearby galaxies. The mean stellar halo mass fraction is 0.009 ± 0.005 with a peak-to-peak scatter of a factor of > 100. Some galaxies in the sample feature strongly structured halos resembling that of M31, but three of the eight galaxies have halos that are completely undetected in our data. We conclude that spiral galaxies as a class exhibit a rich variety in stellar halo properties, implying that their assembly histories have been highly non-uniform. While the outskirts of some galaxies are dominated by halos with the rich substructures predicted by numerical simulations, in other cases the outermost parts of galaxies are simply the extrapolated smooth starlight from enormous stellar disks that closely trace neutral gas morphology out to around 20 scale lengths.

Keywords. galaxies: spirals, galaxies: halos, galaxies: stellar content, techniques: photometric

1. Motivation

A fundamental prediction of hierarchical galaxy formation models in a dark energy-dominated Cold Dark Matter cosmology (ΛCDM) is that all galaxies are surrounded by a vast and complex network of ultra-low surface brightness filaments and streams, the relics of past merger events (Purcell *et al.* 2007; Johnston *et al.* 2008; De Lucia & Helmi 2008; Cooper *et al.* 2013; Pillepich *et al.* 2014). Resolved (star count based) analyses have have revealed the existence of streams and filaments around the Milky Way (e.g. Majewski *et al.* 2003; Belokurov *et al.* 2006; McConnachie *et al.* 2006; Carollo *et al.* 2007; Bell *et al.* 2008) and M31 (e.g. Ibata *et al.* 2001; Ferguson *et al.* 2002; Ibata *et al.* 2007; Richardson *et al.* 2008; McConnachie *et al.* 2009; Gilbert *et al.* 2012). These impressive results provide strong evidence that some massive spiral galaxies formed, at least in part, hierarchically. In the ΛCDM picture many thousands of such streams and filaments combine over time to define galactic extended stellar halos, with the bulk of the material distributed at surface brightnesses well below 30 mag/arcsec^2 (Johnston *et al.* 2008). In contrast to the star-count based results on stellar streams, the detection of these halos has proven elusive. The Hubble Space Telescope has undertaken some very successful deep pencil beam star count surveys of a number of galaxies outside the local group (e.g. the GHOSTS survey; c.f. Radburn-Smith *et al.* 2011 and references therein) but since these stellar halos are very extended (tens of arcminutes for nearby objects), nearby halos

may not be well sampled by pencil beams, and the seemingly much simpler strategy of trying to image them directly using ground-based telescopes is quite attractive. Many such studies have claimed detections of the extended low surface brightness stellar halos of galaxies on the basis of direct imaging, but these claims are now controversial, with recent investigations dismissing these 'halos' as simply being scattered light. This point was first made by de Jong in 2008, and the putative detection of low surface brightness stellar halos from unresolved imaging has recently been the subject of two exhaustive investigations by Sandin (2014, 2015), who concludes that most claimed detections are spurious.

2. Why is low surface brightness imaging such a hard problem?

The faintest galaxies detected at present are about seven magnitudes (over a factor of 600) fainter than the faintest galaxies studied during the 'photographic era' of astronomy prior to the mid-1980s. It is therefore quite remarkable that over this same period of time there has been essentially no improvement in the limiting surface brightness of deep imaging observations of galaxies. (For example, the low surface brightness limits presented in Kormendy & Bahcall 1974 are quite impressive even by modern standards). This is because low surface brightness imaging is not usually limited by photon statistics or by spatial resolution. Instead, it is limited by imperfect control of systematic errors.

The most obvious systematics are instrumental, and these find their origin in the optical train (e.g. in scattering and internal reflections) or in the detector (e.g. in imperfect flat fielding and dark-current subtraction). Once these have been mastered, nature provides a host of complications external to the imaging system. Some of these complications are well-known, such as variability in the sky background introduced by airglow lines in the upper atmosphere, and some are not so well-known, such as the non-negligible structure of the telescopic point-spread function on spatial scales of tens of arcminutes (King 1971; Racine 1996; Sandin 2014). One must also reckon with very significant sources of low surface brightness contamination that have an extraterrestrial origin, such as galactic cirrus (likely to be the dominant systematic in many cases) and the unresolved sources making up the extragalactic background light (Bernstein 2007).

The reader will probably agree that this is a distressingly long list of systematics that one needs to worry about in order to undertake a search for galactic stellar halos. Yet, it gets worse, since in most cases, imperfect corrections made for the systematics just noted will result in *false positive* detections of low-surface brightness galactic stellar halos. It is not hard to undertake deep imaging observations that 'find' galactic stellar halos that in reality may or may not exist. *The true challenge is to hit the required depth with the precision needed to only find halos when they really do exist.* But in spite of (or perhaps because of) these issues, the low surface brightness Universe is a treasure trove of almost totally unexplored astrophysical phenomena: galactic stellar halos are only the beginning. If one could 'crack' the systematics preventing us from getting down to really low surface brightness levels, new avenues would be opened up in an large range of subjects over an immense range of scales from the Solar System all the way out to the Cosmic Web.

3. The Dragonfly Telephoto Array

The Dragonfly Telephoto Array (Abraham & van Dokkum 2014) was designed to break through most of the challenges we have just noted in order to explore the low surface brightness universe with high precision. The most intractable problem in low surface brightness imaging is scattering in the optical train, typically from faint stars in the

https://doi.org/10.1017/S1743921316012291 Published online by Cambridge University Press

Figure 1. One of the two 24-lens arrays comprising the 48-lens Dragonfly Telephoto Array. The lenses are co-aligned and the full array is equivalent to a 1m aperture $f/0.39$ refractor with a 2 deg x 3 deg field of view. The arrays are housed in domes at the New Mexico Skies observatory, and operate as a single telescope slaved to the same robotic control system. The lenses are commercial 400mm Canon USM IS II lenses that have superb (essentially diffraction limited) optical quality. This particular lens has very low scatter on account of proprietary nanostructure coatings on key optical surfaces (see Abraham & van Dokkum 2014 for details). Each lens is affixed to a separate CCD camera and both are controlled by a miniature computer attached to the back of each camera that runs bespoke camera and lens control software that we have made publicly available on a GitHub repository. In the latest incarnation of Dragonfly, each lens is self-configuring and is controlled by its own node.js JavaScript server in an 'Internet of Things' configuration that provides a RESTful interface. Growing the array is done by simply bolting a new lens onto the onto the array and plugging in network and power cables.

field, though sometimes from bright stars outside the field (see Slater *et al.* 2009 for a beautiful investigation of the sources of scatter). Because this scattering originates in several of the basic design trades that make large telescopes possible (e.g. an obstructed pupil and reflective surfaces that have high-frequency micro-roughness that backscatters into the optical path and pollutes the focal plane), Dragonfly has an unobstructed pupil and no reflective surfaces at all. The array builds up its effective aperture by multiplexing the latest generation of high-end commercial telephoto lenses that use nano-fabricated coatings with sub-wavelength structures to yield a factor of ten improvement in wide-angle scattered light relative to other astronomical telescopes (see Sandin 2015 for a comparison). The array is designed to increase in aperture with time, and over the last two years a 48-lens Dragonfly array has been assembled gradually in New Mexico as a collaboration between the University of Toronto, Yale and Harvard. In its current configuration (half of which is shown in Figure 1) Dragonfly is equivalent to a 1m aperture $f/0.39$ refracting telescope with a six square degree field of view and optical scattering an order of magnitude lower than conventional telescopes.

Because several of the key systematics lie outside of the array, the operational model for using Dragonfly is in some ways as innovative as the hardware. When investigating galaxy halos, the array points only at locations pre-determined (on the basis of IRAS imaging) to have low galactic cirrus contamination, and the array operates in a fully autonomous robotic mode that tracks atmospheric systematics in real time. This is important because once one has greatly reduced the wide-angle scatter inherent to the instrument, the tall pole becomes the atmosphere. The atmospheric component of the wide-angle scatter is variable (a fact noted by Sandin 2014), and our Dragonfly data shows quite clearly that this variability extends down to a timescale of minutes. Dealing with these sorts of 'second order' non-instrumental scattering issues clearly matters – see Figure 2 for an illustrative example†.

† The wide-angle telescopic PSF (the 'stellar auroeole') is not well understood. Its origin has been claimed to be mainly instrumental (e.g. Bernstein 2007), but a very significant fraction is

https://doi.org/10.1017/S1743921316012291 Published online by Cambridge University Press

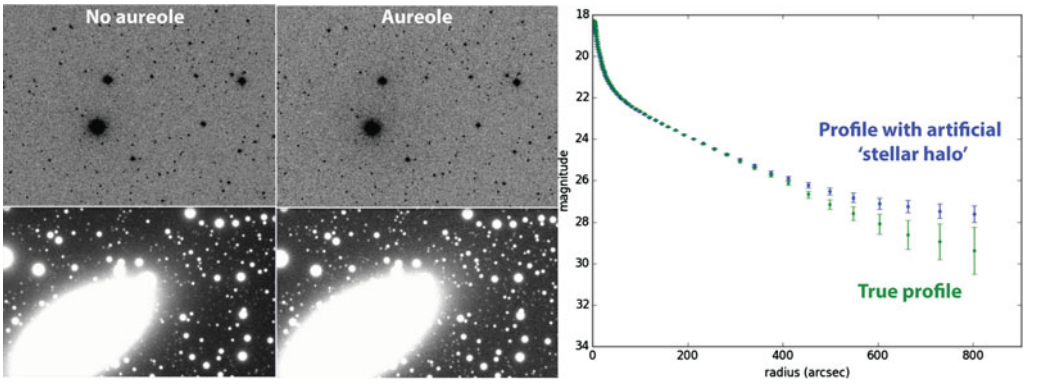

Figure 2. A 'spot the difference' exercise for the reader. This figure shows the results from a simulation intended to explore the impact of variability in the atmospheric component of the wide-angle stellar point-spread function (the 'stellar aureole'). The top panels in the first two columns show 40 arcmin x 60 arcmin regions from single 600s Dragonfly frames with photometric zeropoints differing by 0.1 mag. The intensity of the stellar aureole has been found to correlate with the zeropoint, and investigation of fields with bright stars shows that small variations in the photometric zeropoints of individual frames at this level correspond to fields with PSFs that have significantly different structure in their wide-angle wings. The bottom half of the left two columns show cutouts from simulated observations of a typical target galaxy. The simulation models the results of a $\sim$ 2 hour exposure with Dragonfly, made by stacking 600 frames obtained from 48 lenses on a galaxy with the structural properties of NGC 2841. The images adopt different forms for the wide-angle PSF, with shapes that result in a 0.1 mag difference in the recovered zeropoints. In the left image we have assumed a standard PSF mdel out to $\sim$ 1 arcmin with negligible contribution beyond this scale. The right image shows the corresponding simulation with a stellar aureole included. The prescription for the aureole is taken from Racine (1996). Note that the impact of the aureole is nearly invisible to the eye, except for the merest hint of additional low level scatter. Nevertheless, the aureole has a profound impact on the shape of the surface brightness profile at large radius. The right-hand panel presents the azimuthally-averaged profile of the target galaxy out to a radius of nearly 0.25 degree. Because the impact of short-timescale wide-angle PSF variability is significant, in the Dragonfly pipeline individual frames are automatically calibrated and assessed for image quality as they arrive. In practice around 20% of data frames that appear fine to the eye are dropped from the final stack because of small variations in their photometric zeropoints. See Zhang *et al.* (in preparation) for details.

4. The outskirts of spiral galaxies revealed by Dragonfly

Dragonfly has recently completed a campaign of ultra-deep imaging of 18 nearby galaxies (the Dragonfly Nearby Galaxies Survey; Merritt *et al.* 2016). All results from this campaign were obtained with Dragonfly in its prototype eight and ten lens configurations, where its performance was equivalent to that of a 0.4m $f/1.0$ refractor, and a 0.45m $f/0.9$ refractor, respectively. An analysis of the (essentially absent) stellar halo of M101 using Dragonfly data was presented in van Dokkum *et al.* (2014), and an analysis of the satellite content of M101 appeared in Merritt *et al.* (2014). van Dokkum *et al.* (2015a, b) and van Dokkum *et al.* (2016) show Dragonfly results on ultra-diffuse galaxies in the Coma cluster. Given the subject of this meeting, our main focus here will be to highlight results that have recently appeared in Merritt *et al.* (2016), and which also appeared in abbreviated form in Allison Merritt's poster at this meeting. This paper presents data on the stellar halo mass fractions of the first eight galaxies in the Dragonfly Nearby Galaxies

due to scattering by icy aerosols in the upper atmosphere (a fact well-known to atmospheric physicists; see de Vore *et al.* 2013 for an interesting application of stellar aureole measurements to global warming).

https://doi.org/10.1017/S1743921316012291 Published online by Cambridge University Press

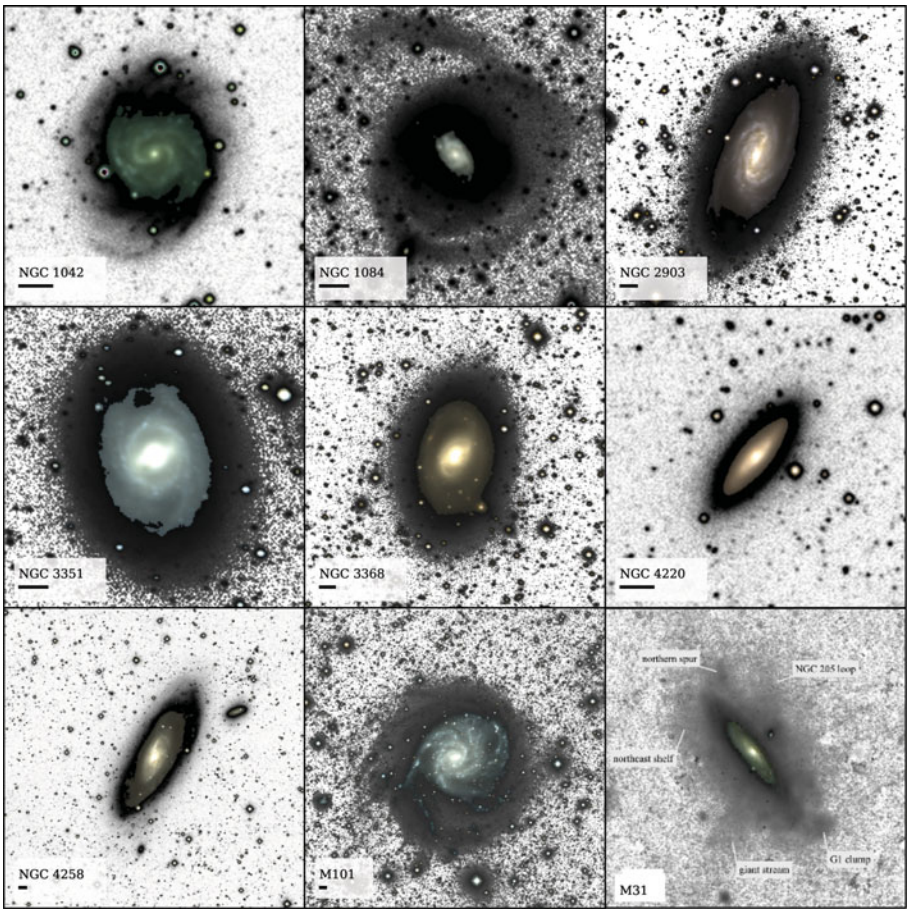

Figure 3. Images of each of the eight galaxies in the sample of Merritt *et al.* (2016). The pseudo-color images were created from g and r band images for the high surface brightness regions, and the greyscale shows the lower surface brightness outskirts. The bottom right panel shows M31, created from a combination of Dragonfly and PAndAS data (McConnachie *et al.* 2009, Carlberg *et al.* 2011) and redshifted to a distance of 7 Mpc (van Dokkum *et al.* 2014). Black lines beneath each galaxy name indicate scales of 1 arcmin. Figure taken from Merritt *et al.* (2016).

Survey. We will also highlight preliminary Dragonfly results on the outer disks of galaxies that were presented in Jielai Zhang's poster at this meeting, and which will be appearing in Zhang *et al.* 2016 (in preparation).

The data shown here are taken from the Dragonfly Nearby Galaxies Survey (Merritt *et al.* 2016), which is a sparse-selected ultra-deep imaging study of 18 galaxies selected on the basis of four criteria: (1) galaxies must have $M_B < -19$ mag; (2) galaxies must be further than 3 Mpc away; (3) galaxies must be located at high galactic latitude within 'holes' of low galactic cirrus determined from IRAS 100μm imaging; (4) galaxies must be visible for extended periods of time with low air mass as seen from New Mexico. No other selection criteria were imposed. The third criterion is interesting, because it turns out that most regions of the high galactic latitude sky are unsuitable for ultra-deep imaging without pre-selection to avoid cirrus contamination.

Deep images of the first eight galaxies (all spirals) in the Dragonfly Nearby Galaxies Survey are shown in Figure 3, together with a 'reconstructed' (by combining star-count

https://doi.org/10.1017/S1743921316012291 Published online by Cambridge University Press

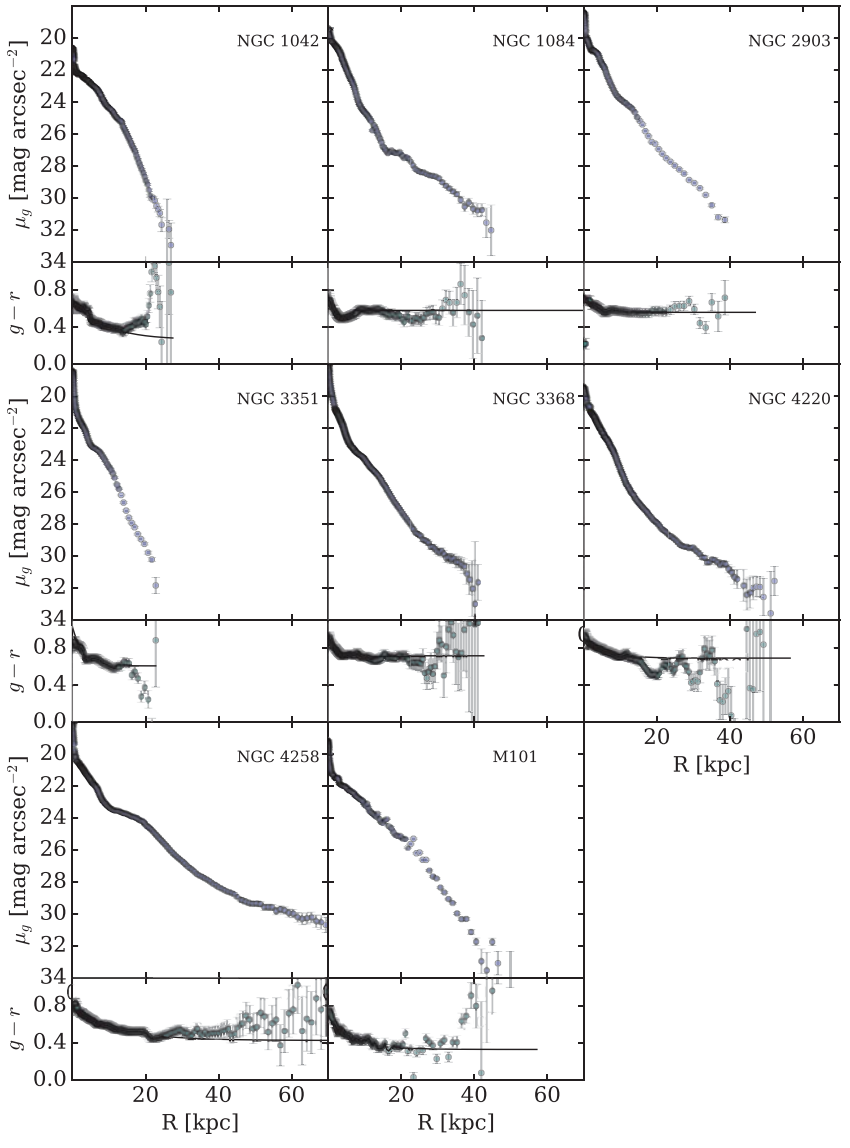

Figure 4. *Top panels* Surface brightness and $g-r$ color profiles (with 1σ error bars) for the first eight galaxies explored in the Dragonfly Nearby Galaxies Survey. Figure taken from Merritt *et al.* (2016).

data in the outskirts and Dragonfly data in the interior) image of M31 as seen at a distance of 7 Mpc using the same instrument. Each image is 30 arcmin on a side. The familiar high surface brightness appearance of the galaxies is shown in color; the low surface brightness outskirts are shown using a grayscale. The galaxies show a remarkable diversity in their low surface brightness structures. Nevertheless, it seems that M31-like halos, characterized by significant substructure, do not appear to be the norm.

Surface brightness profiles corresponding to the galaxies shown in Figure 3 are shown in Figure 4. All profiles extend down to at least 32 mag/arcsec^2, with some stretching down to 34 mag/arcsec^2. We have restricted these profiles to regions with high signal to noise, and have incorporated known systematics into the uncertainty estimates. Since

https://doi.org/10.1017/S1743921316012291 Published online by Cambridge University Press

all of the galaxies are well-studied, Merritt *et al.* (2016) presents careful comparisons between profiles obtained using Dragonfly data and previously published surface brightness profiles for these galaxies. There is an excellent agreement between these profiles in brighter regions where many surveys overlap. Results remain quite consistent until around 29 mag/arcsec^2, at which point relatively little comparison data exists. However, starting at these low surface brightness levels, Dragonfly profiles generally show less evidence for deviations from exponential disks than do profiles from other investigations (e.g. Pohlen *et al.* 2006 and Watkins *et al.* 2014). One exception is NGC 4258, since the Dragonfly observations of this system reveal a very low surface brightness extended red structure. The reader is referred to Merritt *et al.* (2016) for details.

What can one learn from these profiles? Probably their most remarkable characteristic is the fact that only a few galaxies show evidence for prominent upturns at low surface brightness levels that might signal the presence of a stellar halo built up by coalescing substructures. If they existed, substructures from M31-like halos would be expected to dominate the profiles below about 27.5 mag/arcsec^2 (Bakos *et al.* 2012), while the very faint streams predicted by numerical simulations (eg. Johnston *et al.* 2008) would likely dominate profiles below around 30 mag/arcsec^2. While some objects (such as NGC 1084; Martinez-Delgado *et al.* 2010) do show substructures at a level reminiscent of M31, three objects (M101, NGC 1042, and NGC 3351) show no evidence at all for an extended stellar halo — these profiles appear to be dominated by flux from the disk to the limits of our observations.

A complementary approach to understanding the contribution from stellar halos is presented in Figure 5, which shows the stellar halo mass fraction as a function of total stellar mass. The total stellar masses of nearby halos are largely unexplored (with some notable exceptions, such as Seth *et al.* 2007, Bailin *et al.* 2011, Greggio *et al.* 2014, van Dokkum *et al.* 2014, and Streich *et al.* 2015). For concreteness, we define the halo mass fraction to be the stellar mass in excess of a disk+bulge model outside of five half-light radii R_h, a region where the stellar halo should start to contribute significantly (Abadi *et al.* 2006, Johnston *et al.* 2008, Font *et al.* 2011, Cooper *et al.* 2013, Pillepich *et al.* 2015). Given the relatively narrow range in stellar mass explored by these observations ($2-8\times10^{10}M_{\odot}$), the data display a remarkably wide range in stellar halo mass fractions. One of the galaxies in our sample, NGC 1084, has a stellar halo mass fraction of 0.049 ± 0.02 (even larger than that of M31), while, as noted earlier, three others (NGC 1042, NGC 3351, and M101) have stellar halos that are undetected in our data. We measure an RMS scatter of $1.01^{+0.09}_{-0.26}$ dex, and a peak-to-peak span of a factor of > 100. This level of stochasticity is high and certainly exceeds the expectations (Amorisco 2015; Cooper *et al.* 2010, 2013) from numerical simulations (the gray regions shown in the Figure), though they may be qualitatively consistent with variations in the structure and stellar populations of nearby stellar halos observed in both integrated light and star counts studies (e.g. Mouhcine *et al.* 2007; Tanaka *et al.* 2011; Barker *et al.* 2012; Monachesi *et al.* 2015). The former may be contaminated by scattered light, and the latter (based on pencil beams) may not be fairly sampling the halos, so the Dragonfly observations provide a robust baseline for future characterization of the stellar halo mass fraction in luminous nearby spirals.

One possible criticism of the results presented so far is that they are based on analyses of surface brightness profiles. The obvious benefit of using profiles is the increase in signal-to-noise they bring because of averaging along isophotes. Another very useful benefit of profiles is that they decrease the dimensionality of the problem being investigated. However, a potential weaknesses of profiles is their strong sensitivity at large radii to the accuracy of sky background estimates. At a more fundamental level, profiles

https://doi.org/10.1017/S1743921316012291 Published online by Cambridge University Press

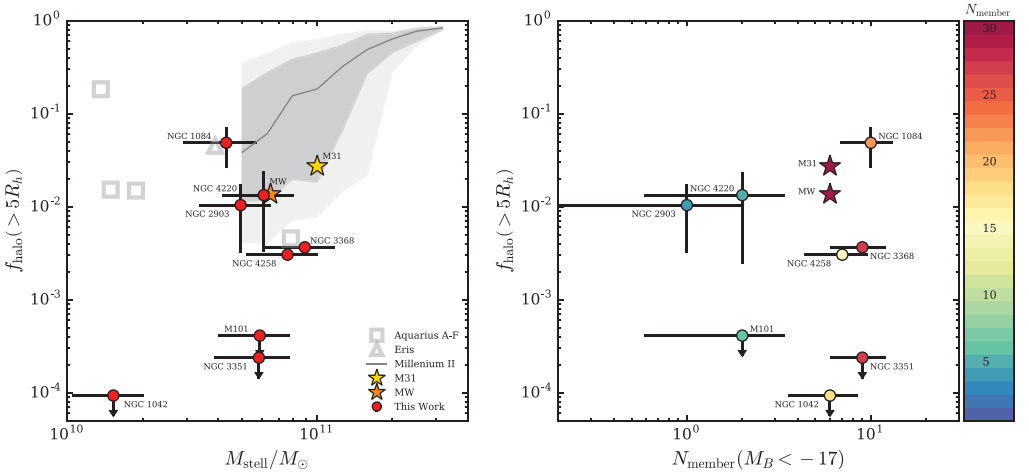

Figure 5. *Left*: The stellar halo mass fractions (and 1σ errors) for the sample in Merritt *et al.* (2016), measured beyond $5R_h$ (red points). Values of $f_{\rm halo}$ for the Milky Way (Carollo *et al.* 2010) and M31 (Courteau *et al.* 2011) are shown for comparison (orange and gold stars, respectively), and have been scaled to the halo mass fraction outside of $5R_h$ assuming the structure of the halo of M31 (Irwin *et al.* 2005, Courteau *et al.* 2011). Predictions of $f_{\rm halo}$, measured over $3 \leqslant r \leqslant 280$ kpc from the Aquarius simulations (Cooper *et al.* 2010); over $r \geqslant 20$ kpc from the Eris simulation (Pillepich *et al.* 2015); and over $r \geqslant 3$ kpc from the Millennium II simulation (galaxies with B/T < 0.9 only; Cooper *et al.* 2013) are indicated by grey open squares, triangles, and shaded region, respectively. *Right*: Environmental richness is parametrized by the number of group members (Makarov & Karachentsev 2011) with $M_B < -17$. The color of each symbol corresponds to the *total* number of known group members for that particular galaxy. The stellar halo mass fractions do not appear to be a function of environment. Figure taken from Merritt *et al.* (2016).

might also be criticized for making strong assumptions about an underlying symmetry in the images. It is therefore interesting to note that many of the most important conclusions obtained so far can be reinforced, at least at a qualitative level, simply by a careful inspection of the images. This is particularly true when the data are viewed in the appropriate panchromatic context. Figure 6 (taken from Zhang *et al.* 2016, in preparation) shows a comparison of GALEX FUV images (top row), radio observations of HI from THINGS (middle row), and ultra-deep g-band Dragonfly imaging (bottom row) for two galaxies with extended UV disks. Lightly-binned Dragonfly images probe down to around 30 mag/arcsec^2 even without the benefit of radial averaging, and at these surface brightness levels it is clear that *at visible wavelengths starlight stretches out to the limits of the HI observations*. In the examples shown, the bulk of the starlight at very large radii is contained within extended disks, rather than in a roughly spherical halo. One suspects that the traditional view that at radio wavelengths disks are about twice as big as they are at visible wavelengths is simply the product of the high sensitivity of the radio data and the limited ability of ground-based telescopes to undertake low surface brightness observations. Careful inspection of Figure 6 shows that at large radii the starlight in the Dragonfly images traces the HI data closely. Smooth starlight also fills in the regions between the UV knots in the GALEX images, which (like the evolved starlight) stretch out to the limits of the radio observations. The existence of evolved disk stars at very large radii is another manifestation of the important problem first highlighted by the existence of XUV disks (Thilker *et al.* 2007): how does one form stars at radii well beyond the bulk of the molecular gas in galaxies, and at locations where disks are at least globally Toomre stable? Certainly local regions of instability can emerge from

https://doi.org/10.1017/S1743921316012291 Published online by Cambridge University Press

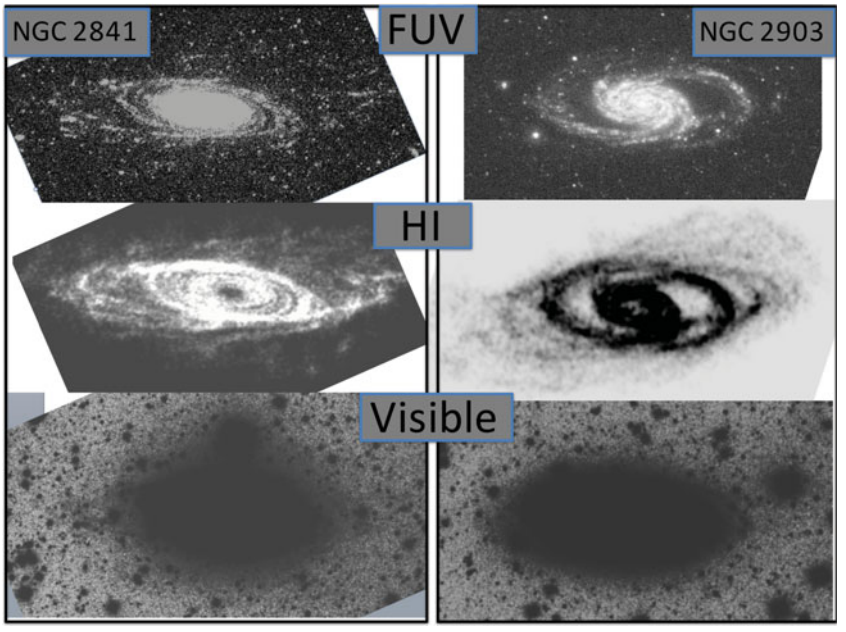

Figure 6. GALEX FUV images (top row), HI observations from THINGS (middle row), and ultra-deep Dragonfly imaging (bottom row) for NGC 2841 (left) and NGC 2903 (right), two systems showing extended UV disks (Thilker *et al.* 2007). Taken from Zhang *et al.* 2016 (in preparation).

dense pockets of gas compressed by turbulence (Elmegreen & Hunter 2006), but what drives the turbulence, and where does the molecular gas come from? In any case, it is amazing to see in these data how, at least in some cases, giant disks rather than stellar halos define the faint outskirts of the galaxies. Is even deeper imaging needed in order to reveal the stellar halos in these systems? This seems likely, but perhaps more ambitious imaging would also reveal a further continuation of the enormous stellar disks already uncovered, as they stretch out to radii at which the disk-halo interface fuels the fire of star formation in the galaxies, and ultimately connects these systems into the cosmic web of primordial gas.

References

Abadi, M. G., Navarro, J. F., & Steinmetz, M. 2006, *MNRAS*, 365, 747
Abraham, R. G. & van Dokkum, P. G. 2014, *PASP*, 126, 55
Amorisco, N. C. 2015, ArXiv e-prints
Bailin, J., Bell, E. F., Chappell, S. N., Radburn-Smith, D. J., & de Jong, R. S. 2011, *ApJ*, 736, 24
Bernstein, R. A. 2007, *ApJ*, 666, 663
Bakos, J. & Trujillo, I. 2012, ArXiv e-prints
Barker, M. K., Ferguson, A. M. N., Irwin, M. J., Arimoto, N., & Jablonka, P. 2012, *MNRAS*, 419, 1489
Bell, E. F., Zucker, D. B., Belokurov, V., *et al.* 2008, *ApJ*, 680, 295
Belokurov, V., Evans, N. W., Irwin, M. J., *et al.* 2007, *ApJ*, 658, 337
Belokurov, V., Zucker, D. B., Evans, N. W., *et al.* 2006, *ApJ*, 642, L137
Carlberg, R. G., Richer, H. B., McConnachie, A. W., *et al.* 2011, *ApJ*, 731, 124
Carollo, D., Beers, T. C., Lee, Y. S., *et al.* 2007, *Nature*, 450, 1020
Carollo, D., Beers, T. C., Chiba, M., *et al.* 2010, *ApJ*, 712, 692

https://doi.org/10.1017/S1743921316012291 Published online by Cambridge University Press

Cooper, A. P., Cole, S., Frenk, C. S., *et al.* 2010, *MNRAS*, 406, 744
Cooper, A. P., D'Souza, R., Kauffmann, G., *et al.* 2013, *MNRAS*, 434, 3348
Courteau, S., Widrow, L. M., McDonald, M., *et al.* 2011, *ApJ*, 739, 20
Dalcanton, J. J. & Bernstein, R. A. 2002, *AJ*, 124, 1328
de Jong, R. S. 2008, *MNRAS*, 388, 1521
De Lucia, G. & Helmi, A. 2008, *MNRAS*, 391, 14
de Vore, J. G., Kristl, J. A., & Rappaport, S. A. 2013, *Journal of Geophysical Research - Atmospheres*, 118, 11, 5679
Elmegreen, B. G. & Hunter, D. A. 2006, *ApJ*, 636, 712
Ferguson, A. M. N., Irwin, M. J., Ibata, R. A., Lewis, G. F., & Tanvir, N. R. 2002, *AJ*, 124, 1452
Font, A. S., McCarthy, I. G., Crain, R. A., *et al.* 2011, *MNRAS*, 416, 2802
Gilbert, K. M., Guhathakurta, P., Beaton, R. L., *et al.* 2012, *ApJ*, 760, 76
Greggio, L., Rejkuba, M., Gonzalez, O. A., *et al.* 2014, *A&A*, 562, A73
Ibata, R., Irwin, M., Lewis, G., Ferguson, A. M. N., & Tanvir, N. 2001, *Nature*, 412, 49
Ibata, R., Martin, N. F., Irwin, M., *et al.* 2007, *ApJ*, 671, 1591
Irwin, M. J., Ferguson, A. M. N., Ibata, R. A., Lewis, G. F., & Tanvir, N. R. 2005, *ApJ*, 628, L105
Johnston, K. V., Bullock, J. S., Sharma, S., *et al.* 2008, *ApJ*, 689, 936
King, I. R. 1971, *PASP*, 83, 199
Kormendy, J. & Bahcall, J. N. 1974, *AJ*, 79, 671
Majewski, S. R., Skrutskie, M. F., Weinberg, M. D., & Ostheimer, J. C. 2003, *ApJ*, 599, 1082
Martínez-Delgado, D., Gabany, R. J., Crawford, K., *et al.* 2010, *AJ*, 140, 962
McConnachie, A. W., Chapman, S. C., Ibata, R. A., *et al.* 2006, *ApJ*, 647, L25
McConnachie, A. W., Irwin, M. J., Ibata, R. A., *et al.* 2009, *Nature*, 461, 66
Merritt, A., van Dokkum, P. G., & Abraham, R. 2014, *ApJLett*, 787, L37
Merritt, A., van Dokkum, P. G., Abraham, R., & Zhang, J. 2016, arXiv:1606.08847
Mihos, J. C., Harding, P., Spengler, C. E., Rudick, C. S., & Feldmeier, J. J. 2013, *ApJ*, 762, 82
Monachesi, A., Bell, E. F., Radburn-Smith, D., *et al.* 2015, ArXiv e-prints
Monachesi, A., Bell, E. F., Radburn-Smith, D. J., *et al.* 2013, *ApJ*, 766, 106
Mouhcine, M., Rejkuba, M., & Ibata, R. 2007, *MNRAS*, 381, 873
Pillepich, A., Madau, P., & Mayer, L. 2015, *ApJ*, 799, 184
Pillepich, A., Vogelsberger, M., Deason, A., *et al.* 2014, *MNRAS*, 444, 237
Pohlen, M. & Trujillo, I. 2006, *A&A*, 454, 759
Purcell, C. W., Bullock, J. S., & Zentner, A. R. 2007, *ApJ*, 666, 20
Racine, R. 1996, *PASP*, 108, 699
Radburn-Smith, D. J., de Jong, R. S., Seth, A. C., *et al.* 2011, *ApJS*, 195, 18
Richardson, J. C., Ferguson, A. M. N., Johnson, R. A., *et al.* 2008, *AJ*, 135, 1998
Seth, A., de Jong, R., & Dalcanton, J., GHOSTS Team. 2007, in IAU Symposium, Vol. 241, IAU Symposium, ed. A. Vazdekis & R. Peletier, 523–524
Sandin, C. 2014, *A&A*, 567, 97
Sandin, C. 2015, A&A, 577, A106
Seth, A. C., Dalcanton, J. J., & de Jong, R. S. 2005, *AJ*, 130, 1574
Slater, C. T., Harding, P., & Mihos, J. C. 2009, *PASP*, 121, 1267
Streich, D., de Jong, R. S., Bailin, J., *et al.* 2015, ArXiv e-prints
Tanaka, M., Chiba, M., Komiyama, Y., Guhathakurta, P., & Kalirai, J. S. 2011, *ApJ*, 738, 150
Thilker, D. A., Bianchi, L., Meurer, G., *et al.* 2007, *ApJSupp*, 173, 538
van Dokkum, P. G., Abraham, R., & Merritt, A. 2014, *ApJ*, 782, L24
van Dokkum, P. G., Abraham, R., Brodie, J., *et al.* 2016, arXiv:1606.06291
van Dokkum, P. G., Romanowsky, A. J., Abraham, R., *et al.* 2015, *ApJLett*, 804, L26
van Dokkum, P. G., Abraham, R., Merritt, A., *et al.* 2015, *ApJLett*, 798, L45
Vlajić, M., Bland-Hawthorn, J., & Freeman, K. C. 2011, *ApJ*, 732, 7
Watkins, A. E., Mihos, J. C., & Harding, P. 2016, ArXiv e-prints
Watkins, A. E., Mihos, J. C., Harding, P., & Feldmeier, J. J. 2014, *ApJ*, 791, 38